

Lateral attenuation of aircraft sound levels over an acoustically hard water surface: Logan airport study

Gregg G. Fleming,^{a)} David A. Senzig,^{a)} and John-Paul B. Clarke^{b)}

(Received 2001 March 07; revised 2001 October 31; accepted 2001 November 05)

A noise measurement study was conducted at Logan International Airport in Boston, Massachusetts, during the summer of 1999 to examine the applicability of currently available mathematical models of lateral sound attenuation. Analysis of the data collected revealed that lateral attenuation is a function of the location of the engines on the aircraft, i.e., tail-mounted versus wing-mounted. Attenuation for aircraft with tail-mounted engines was found to agree with the published literature, as well as that included in existing aircraft noise models. Attenuation for aircraft with wing-mounted engines was found to be less than that documented in the literature. This lower lateral attenuation for aircraft with wing-mounted engines results in a general under-prediction of side-line noise by the existing noise models. © 2002 Institute of Noise Control Engineering.

Primary subject classification: 76.1.1.3; Secondary subject classification: 24.4

1. INTRODUCTION

Accurate modeling of the lateral attenuation of sound is essential for accurate prediction of aircraft noise. "Lateral attenuation" contains many aspects of sound generation and propagation, including ground effects (sometimes referred to as excess ground attenuation), shielding and reflections from aircraft structures, aerodynamic refraction of sound, jet shielding due to closely-spaced jet engine exhausts, as well as other factors. Although much work has been done to quantify lateral attenuation as it relates to aircraft,¹⁻⁵ there continue to be wide discrepancies between predicted and measured noise levels, especially for situations involving sideline receptors and aircraft at low altitudes, where lateral attenuation effects can be substantial. These discrepancies, which tend to be larger for many of the more modern jet aircraft, are an even greater issue at airports surrounded by acoustically varying land cover, e.g., coastal airports surrounded by a mix of both acoustically hard water and acoustically soft grass. These discrepancies exist because most aircraft noise prediction models rely on algorithms that assume propagation over acoustically soft ground, and are based on data from older jet aircraft.

The Acoustics Facility at the United States Department of Transportation John A. Volpe National Transportation Systems Center (Volpe Center) and the Massachusetts Institute of Technology (MIT) conducted a noise measurement study at Logan International Airport in Boston, Massachusetts, during the summer of 1999. The goal of this study, funded by the National Aeronautics and Space Administration (NASA)

Langley Research Center (LaRC), was to examine the applicability of currently available mathematical models of lateral attenuation. The results of that measurement study are presented in this paper.

A. Background

The lateral attenuation algorithms currently deployed in the Federal Aviation Administration (FAA) Integrated Noise Model (INM) are based on the methods described in the Society of Automotive Engineers (SAE) Aerospace Information Report (AIR) 1751.¹ Specifically, SAE AIR 1751 contains two algorithms: one used to compute attenuation due to air-to-ground propagation (for airborne aircraft); and one for computing attenuation due to ground-to-ground propagation (for aircraft taxiing, landing or in takeoff-ground roll). Within the INM, up to and including Version 6.0,^{6,7} these two field-measurement-based (empirical) equations are used to compute the ground effects for all commercial aircraft. Similar empirical equations are used for military aircraft.

SAE AIR 1751, released in 1981, is based on data measured in the 1960s and 1970s. The majority of the aircraft represented in the AIR were equipped with low-bypass ratio jet engines. In particular, the data set is dominated by a single type of jet aircraft, the Boeing Model 727-100 (B727-100), which first flew in 1963. The inclusion of the SAE AIR 1751 lateral attenuation algorithms in the INM leads to two generalizations that lower the accuracy of the model: (1) lateral attenuation data dominated by one type of aircraft are applied to the entire aviation fleet equally; and (2) propagation effects over acoustically hard terrain are not considered. The latter generalization is a major weakness at airports in coastal areas where airports are typically surrounded by a mixture of acoustically hard (water) and acoustically soft (grass) terrain. Consequently, in 1997 the INM development team initiated the task of revising the lateral attenuation algorithms within the model.

^{a)} U.S. Department of Transportation, Research and Special Programs Administration, John A. Volpe National Transportation Systems Center, Acoustic Facility, DTS-34, Cambridge, MA 02142-1093, USA; E-mail: Fleming@VOLPE.DOT.GOV.

^{b)} Massachusetts Institute of Technology, Department of Aeronautics and Astronautics, 77 Massachusetts Avenue, Room 33-314, Cambridge, MA 02139-4307, USA.

At the most fundamental level, lateral attenuation of aircraft noise comprises two basic physical phenomena: engine installation effects and ground attenuation effects. Engine installation effects, which are implicit in the SAE AIR 1751 algorithms, include shielding and reflections from aircraft structures, aerodynamic refraction of sound, and jet shielding due to closely-spaced jet engine exhausts. These engine installation effects are not well understood. In the latest version of the United States Air Force's NOISEMAP computer program for assessing the noise impact in the vicinity of military installations, engine installation effects are neglected and modeling of lateral attenuation is based solely on ground attenuation effects.³ However, the data that were used in the development of SAE AIR 1751 seem to indicate that for some commercial aircraft, e.g., the B727, engine installation effects may be important, depending upon source-to-receiver geometry. Conversely, ground attenuation effects account for the introduction of an impedance boundary, in this case the ground surface, into a given aircraft-to-receiver geometry. This study examines both of these components of lateral attenuation, with a primary focus on the less understood engine installation effects.

Various institutions have sought to update the existing lateral attenuation algorithms in the standard noise models. The Department of Operational Research and Analysis of the National Air Traffic Services Ltd. (NATS) in London has collected a large database of aircraft departure data at London's Gatwick Airport.⁸ These data were collected between 1996 and 1999. The data show that lateral attenuation appears to be a function of aircraft geometry, i.e., the specific placement of engines and structural components of an aircraft influences lateral attenuation.

B. Objectives

The primary objectives of the Logan Study were to:

- assess the accuracy of the new ground effects regressions developed for future inclusion in the FAA's INM;
- examine and, if possible, quantify the engine installation component of the lateral attenuation; and
- quantify the error in utilizing SAE AIR 1751 for computing fleet-wide lateral attenuation and provide a database to assist in the process of updating SAE AIR 1751.

A further objective was to compare data collected in this study with the data collected in the previously mentioned NATS study.

Since Logan is a coastal airport, the study concentrated on the assessment of the ground effects regressions developed for propagation over an acoustically hard surface. These ground effects regressions are detailed extensively in Ref. 9. Also, because ground effects for propagation over an acoustically hard surface are more predicable than for propagation over an acoustically soft surface, engine installation effects could be more easily quantified.

C. Measurement sites

Simultaneous acoustic measurements were made at three locations along the Winthrop, Massachusetts shoreline. As Fig. 1 shows, these locations consisted of a centerline

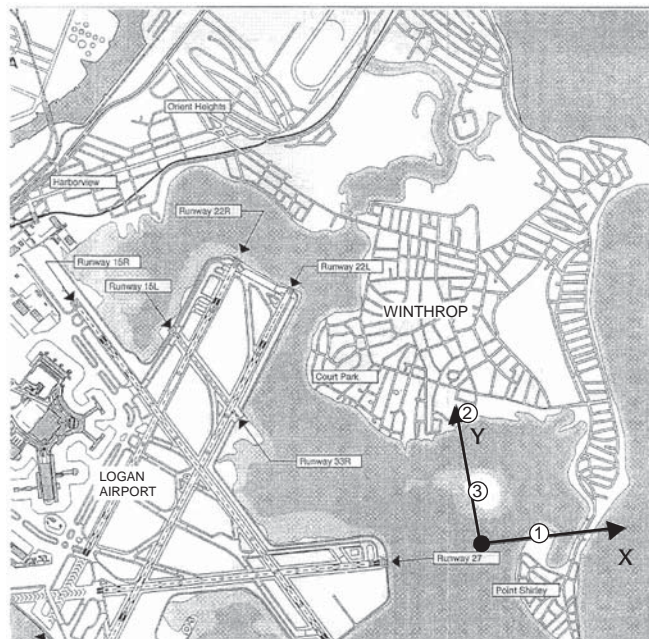


Fig. 1 – Measurement site.

reference site located directly underneath the nominal flight track for departures and approaches on Runway 9/27 (Point 1), a second site located about 915 m (3,000 ft) to the north of the nominal track (Point 2), and a third site located on Snake Island in Boston Harbor (Point 3). Two microphones were deployed at each location. The first microphone was installed at a height of 1.5 m (5 ft) while the second microphone was installed at a height of 4.5 m (15 ft). The second microphone was positioned directly above the first microphone. The microphone assemblies at sites 2 and 3 were directly adjacent to the shoreline. Thus, both sites had the same effective impedance. The primary benefit of having two sites, both surrounded by water, on the same perpendicular line from the flight track was that the consistent surface impedance would allow for more simplistic modeling of the ground effect, thus facilitating easy data reduction.

2. INSTRUMENTATION

Figure 2 shows a schematic of the acoustic measurement system. Reference 10 presents detailed technical specifications for the acoustic measurement system and for the time-space-position information (TSPI) system. Both are briefly described below along with the instrumentation used to survey the measurement sites and establish a local coordinate system, and other ancillary instrumentation

A. Microphone, preamplifier, and windscreen

The Brüel and Kjær (B&K) Model 4155 microphones used in the current study are electret condenser microphones. These microphones utilize a diaphragm of pure nickel, which is coated with a protective quartz film. The microphone

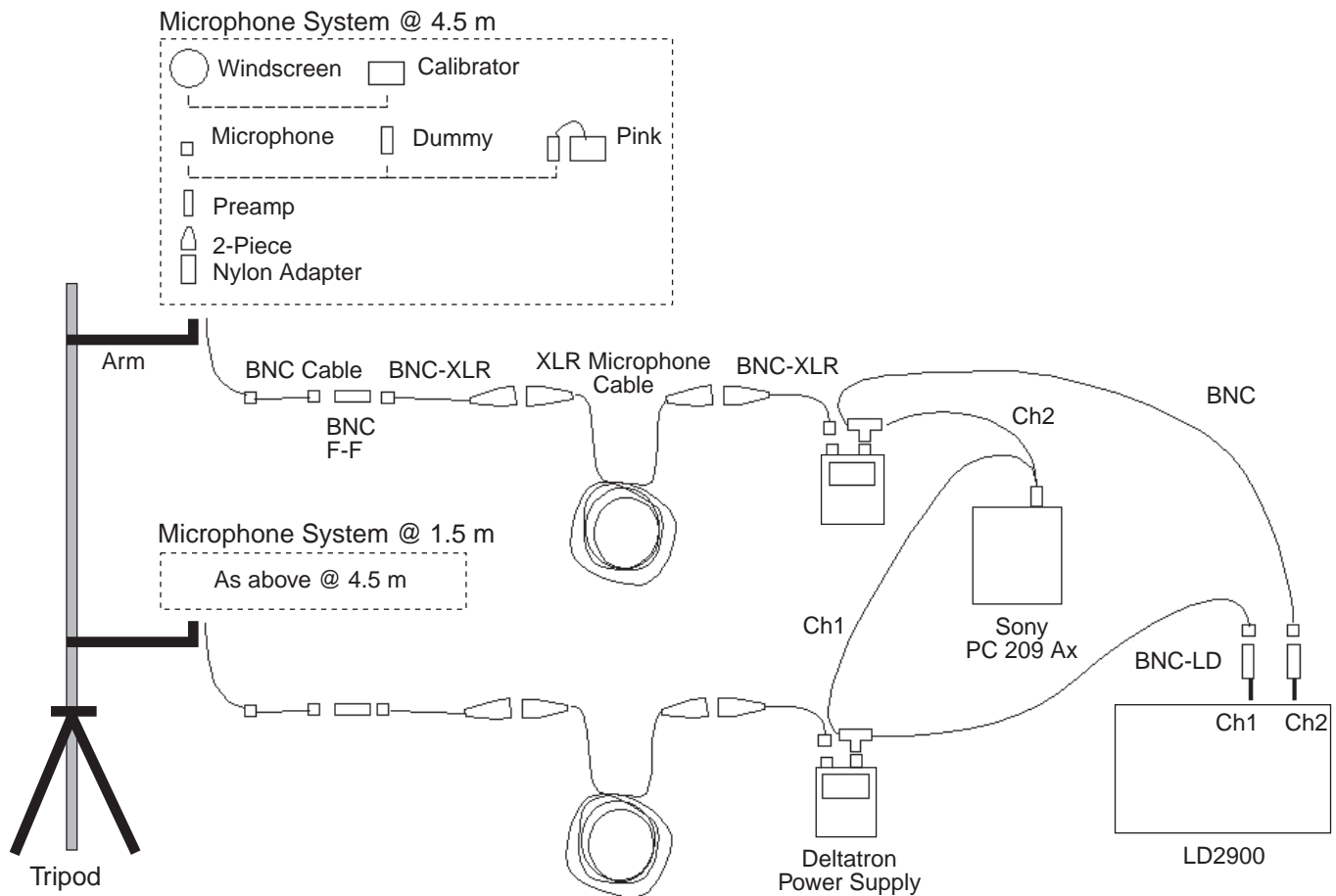


Fig. 2 – Acoustic measurement system.

backplate is made of a corrosion-resistant high-nickel alloy which carries a negatively charged layer. With this design the microphone is able to maintain its own polarization (often referred to as a *pre-polarized* design). Pre-polarization allows the electret microphone to function as a *closed system* with regard to humidity, thus eliminating a concern at the coastal locations and summertime measurement period of the current study. Additionally, B&K Model 2671 preamplifiers and Model WB 1372 power supplies were employed at each site. A B&K Model 0237 90 mm (3.5 in) foam windscreen was placed atop each microphone to reduce the effects of wind-generated noise on the microphone diaphragm. By reducing such noise, the signal-to-noise (S/N) ratio of a sound measurement is effectively improved.

B. Spectrum analyzer

Each microphone/preamplifier was connected via 30.5 m (100 ft) of cable to a Larson Davis Laboratories (LDL) Model 2900, two-channel, one-third octave-band analyzer (LDL2900) set-up at each measurement location. Each channel of the LDL2900 was setup to continuously measure and store, at 1/4-second time intervals, the unweighted, slow, linearly averaged one-third octave-band spectral time history. In this configuration the LDL2900 (with 4 Megabytes of random access memory) is capable of storing slightly over one half hour of data. During data collection, the LDL2900

at each site was turned on at the audible start of each event, left on throughout the event, and shut off either at the conclusion of the event or when ambient noise became audible during the event of interest. The contents of internal memory were periodically transferred to a floppy disk for off-line reduction and analysis (see Section 3). This data download was only performed during periods when no events of interest were taking place.

C. Digital audio tape recorder

Each microphone/preamplifier was also connected to a Sony Model PC208Ax digital audio tape (DAT) recorder. The DAT recorder was set up to operate in a four-channel recording mode. The two microphones/preamplifiers were connected to the first two channels. In this configuration, each 90 m (295 ft) tape provided slightly more than 3 hours of recording time. Unlike the LDL2900, the DAT recorder was setup to record continuously throughout a measurement day. Universal Coordinated Time (UTC) was recorded from a True Time Model 705 time code generator on the third DAT channel. The fourth channel of the DAT was unused. The tape recorded data enabled repeated playback and analysis of the collected data, including the option of subsequent narrow-band analysis, if necessary.

D. Acoustic observer log

A manual acoustic observer log was maintained to provide a time synchronized history of observed aircraft activity. Ambient noise conditions were also noted on the log sheets.

E. Meteorological instrumentation

In addition to the acoustical instrumentation, a Qualimetrics® Transportable Automated Meteorological Station (TAMS) was set up at each of the three measurement locations. The TAMS measured temperature, relative humidity, wind speed and direction, and ambient atmospheric pressure at one-second intervals. Wind speed and direction were 10-second running averages.

F. Time-space-position instrumentation

The time-space-position information (TSPI) system includes two digital video camera subsystems and their supporting accessories. Each subsystem recorded aircraft events onto video tape that was subsequently processed to determine the aircraft's position versus time throughout the event. Each subsystem consisted of a Canon Optura® digital video camera with a wide-angle lens and the supporting hardware to enable field calibration of the system. The supporting hardware included portable video targets, a camera support structure that permitted the camera to be rotated about all three axes, a laser and laser mounting structure, and equipment to accurately determine the geometry of the calibration coordinate system.

G. Survey instrumentation

A site survey was conducted using a differential Global Positioning System (dGPS) which was designed and developed by the Volpe Center around two single-frequency (commonly referred to as L1) NovAtel® Model RT20E GPS receivers and two GLB® Model SNTR 150 transceivers which facilitate remote communication between the two GPS receivers.¹¹ The two 25-Watt GLB transceivers were tuned to a frequency of 136.325 KHz. The dGPS system also contained a Graphical User Interface (GUI) and supporting software that was tailored for use during aircraft noise certification tests.

The dGPS system was used to determine a coordinate system for the measurement instrumentation and the aircraft (see Fig. 1). This coordinate system was also used in the data processing and analysis. The coordinate system used was defined with the positive X-axis running under the departure centerline from Runway 09, the positive Y-axis in the direction of the Snake Island and Corinha Beach measurement locations (positions 3 and 2 in Fig. 1, respectively), and the positive Z-axis vertically up.

H. OTHER INSTRUMENTATION

B&K Model 4231 sound calibrators were used to establish and check the sensitivity of the entire acoustic instrumentation system (i.e., microphone, preamplifier, cables, spectrum analyzer and DAT). The Model 4231 produces a user-selectable 114 dB sound pressure level at 1 kHz.

Time synchronization of all pertinent instrumentation in the measurement chain was performed using a True Time Model 705 time code generator as reference. The Model 705 has a built-in GPS receiver, thus facilitating automatic time synchronization at all remote measurement sites. Universal Coordinated Time (UTC) with a local hour offset was used as the time base for the study. In particular, the LDL2900, the DAT, the meteorological instrumentation, and the video system were all synchronized to facilitate accurate data reduction and analysis. The radar tracking system at Logan is also synchronized to UTC, thus facilitating the coordination of acoustical, meteorological and flight track data, if coordination with the radar system data was subsequently deemed necessary.

During measurements, a Radio Shack Model PRO-63 Event Scanner was continuously tuned to the frequency of the Logan control tower. Monitoring of aircraft-to-tower communications greatly assisted in the process of identifying aircraft types.

Motorola Radius GP300 FM radios were utilized for communication between the test director and personnel at each measurement site.

3. FIELD MEASUREMENTS

Field Measurements were conducted in late June and mid July, 1999, between 9:00 a.m. and 3:00 p.m. on days when Runway 9/27 was in use and winds were below 15 knots (17 miles per hour). The measurement days were June 23, June 24, June 29, June 30, July 12, July 14 and July 16.

The measurement team consisted of three groups of two people to operate the acoustic measurement systems, and two additional people to operate the two video cameras. One of the video camera operators doubled as the test director, who would alert the teams to upcoming aircraft events and would also provide data on aircraft types, flight number and ownership.

During a typical measurement event, personnel at the acoustic measurement sites were responsible for starting and ending operation of the LDL2900 and logging pertinent event information such as time of day, event duration, possible contamination, etc. This was done so that individuals at each site could make decisions based on the ambient levels and event levels at each site.

A. Acoustic site setup

At the start of a typical measurement day, each microphone system, including preamplifier and windscreen, was attached to a telescoping tripod mast positioned as close as possible to the shoreline (in the case of the sideline measurement sites) and directly underneath the nominal flight track (in the case of the centerline measurement site). Thus, the masts at sites 2 and 3 were moved throughout the testing period in response to tidal shifts. At all times, each mast was adjusted to locate one microphone diaphragm at a height of 1.5 m (5 ft) and the other directly over the first at a height of 4.5 m (15 ft) above the local surface. The microphones were oriented for grazing incidence (+/-30 degrees) to the expected nominal flight track.

This orientation protocol was used to ensure consistency with the rigid requirements of aircraft noise certification, which call for grazing incidence.

The LDL2900, DAT, and acoustic observer were positioned in full view of the microphone location, but at a distance of approximately 30.5 m (100 ft) to eliminate data contamination due to observer activity.

The meteorological instrumentation was positioned approximately 7.5 m (25 ft) from the observer location. The meteorological sensors were placed at approximately 3 m (10 ft) above the ground.

The clocks of all pertinent instrumentation (the LDL2900, DAT, meteorological system, and video system) were set using the True Time Model 705 time code generator. UTC, with a local hour offset, was received and translated to a standard analog time code format and recorded on a separate channel of each DAT recorder.

With all electrical components of the acoustic measurement system connected, a sound level calibration and complete acoustic check-out of the system was performed. The windscreen was installed atop each microphone/preamplifier combination and continuous DAT recordings and meteorological data collection were initiated. As previously mentioned, aircraft sound level measurements with the LDL2900 were obtained on a per-event basis.

B. TSPI site setup

At the start of a typical measurement day, each video tripod and three-axis head were assembled and positioned at the two sites noted in the dGPS survey (sites 1 and 2 in Fig. 1). The two video targets were assembled at their known coordinate locations. The heights of targets above the ground were noted for use in later computer processing. The video camera was started and the UTC time code was recorded. The camera, still running, was mounted on the tripod assembly.

Next, the video camera located at Corinha Beach (site 2) was rotated on its three-axis head so that the left-of-center video target was in the center of the view finder image. The video camera at Pt. Shirley (site 1) was rotated clockwise 90 degrees about the roll axis, then pitched up 45 degrees. This was done to maximize the field of view at Pt. Shirley. With the wide angle lens installed, the Optura camera has a field of view of about 90 degrees in the nominally horizontal direction and about 60 degrees in the nominally vertical direction. At Pt. Shirley, the horizontal and vertical directions were switched by rolling the camera 90 degrees. Because the nominal flight path for Runway 9/27 was directly over Pt. Shirley, pitching the camera upwards to 45 degrees allowed the camera to record departing aircraft from the time they left the runway until they passed almost directly overhead.

C. Measurement procedures

Upon identification of an event by the test director, the acoustic personnel began data capture on the LDL2900 as soon as the event was audible. During data capture, acoustic personnel logged pertinent observations (e.g., noise contamination due to aircraft taxiing, unidentified airport

sources, and localized community sources). When the event was no longer audible, or when ambient noise began to influence the event noise levels, the LDL2900 was stopped. The test director also coordinated the numbering and identification of aircraft events.

Throughout measurements, periodic checks were performed on the acoustical, meteorological and video instrumentation for the following: available battery power, remaining internal memory for devices with internal data storage (LDL2900 and meteorological system), and remaining tape in the case of the DAT recorder and the video system.

D. Measurement system dismantling

At the completion of a typical measurement day, a post-measurement sound level calibration of the entire acoustical system was performed and any drift from the initial calibration was documented. In addition, the internal clocks of the LDL2900, DAT, meteorological system, and TSPI instrumentation were compared with the master clock, and any time drift documented. The video camera UTC time code taping was repeated. The sound level data recorded in the LDL2900 were downloaded to a laptop computer and stored.

4. DATA REDUCTION

A suite of computer programs was written to facilitate data reduction. The programs require three primary input data sets: acoustical data, video data, and meteorological data. For each measurement event: the acoustic data comprise time-stamped one-third octave-band spectral time histories as recorded by the LDL2900 in binary format; the video data comprise video recorded in the field; and the meteorological data comprise time-stamped temperature, relative humidity, atmospheric pressure, wind speed and direction in ASCII format.

In addition to data management, these programs calculate the known propagation effects from the aircraft to each of the microphone locations, normalizes these data to the 1.5 m (5 ft) reference microphone at Pt. Shirley (site 1), and returns the level difference between the normalized data and the actual reference. This difference is the “residual” discussed in subsequent sections. The known propagation effects include spherical spreading, atmospheric absorption and ground effect. Spherical spreading was computed assuming point source propagation [$20\log_{10}(d/d_{ref})$]. The atmospheric absorption of sound was computed using two different algorithms, those presented in SAE Aerospace Information Report 866a and the International Standard Organization’s ISO 9613-1. The data corrected using ISO 9613-1 are presented in subsequent sections. Ground effects were computed using the algorithms of Embleton, Piercy, and Daigle, i.e., the EPD algorithm.¹²

In order to accomplish the defined objectives, sound measurements were analyzed for a short time period around the instant when each aircraft was at the Closest Point of Approach (CPA) to the individual microphone locations. In this study, the symbol used for the A-weighted sound level emitted at the point of closest approach is L_{CPA} .

Examining L_{CPA} provides several benefits. The first benefit is that issues related to directivity are eliminated. At CPA for all three microphone locations, the angle from the centerline of the aircraft to the microphone is always 90 degrees. The second benefit is that timing issues are simplified. With a known three-dimensional flight path vector, calculation of the propagation time from the aircraft to each individual microphone is straightforward. The third benefit is that the noise at CPA is the noise at a single instant of time; the received noise can be analyzed knowing the exact geometry between the aircraft and the receiver. The fourth benefit is that, during the short time period considered, the aircraft undergoes no power setting or flap changes.

A. Data culling process

The first step in the reduction of the data was the decision to concentrate the analysis on departure data, not arrival data. Departure events significantly outnumber arrival events. This, combined with the lower signal-to-noise ratio of the arrival data and the inability to state with confidence that no power setting changes occur in the final segment of the approach, led to the decision to forego analysis of the arrival data.

Figure 3 shows the entire set of data collected for departure events. This data set represents 339 total departure events measured by the five microphones, which were corrected to the reference microphone. The data points are plotted as a function of elevation angle. The elevation angle was the aircraft's angle above the horizon as seen from the particular microphone. The dependent axis represents the difference between the as-measured corrected data observed at each of the five microphones and the reference microphone. "Corrected" for the five measurement microphones means the 1.25 second, energy-averaged spectra at CPA were corrected to the same distance as the CPA distance associated with the reference microphone. Correction for these five microphones involves spherical spreading, atmospheric absorption, and ground effect. "Corrected" for the reference microphone involves only the application of the EPD ground

effects algorithm to remove the ground reflection effect present in the measured sound. All data were A-weighted during the analysis. The label on the dependent axis is labeled 'residual.' The residual is believed to be synonymous with the engine installation effect, since neglecting meteorological effects, all other physical effects in the measured data have been accounted for in the correction process.

The data presented in Fig. 3 were culled using two criteria for removing potentially contaminated data. The first criterion was to remove all events that had a recorded wind speed of 16.1 km/hr (10 mph) or greater at any of the three meteorological stations any time in the event. The second criterion was to remove all events that had a possibility of a power setting change before passing over Pt. Shirley. Lastly, only the data for a limited number of aircraft types were used in the final analysis, to avoid working with aircraft types that did not have a large sample population.

B. Aircraft types

After the culling process, six aircraft types were considered to have an adequately large population for inclusion in the analysis. These six types were the B727, DC9, MD80, B737 (with CFM series engines), B757, and A320. All other aircraft types were excluded from further analysis. Note that within each of these types there are large possible variations in weights, engine thrust settings, and, for the B757 and A320, different engines. These differences do not affect this analysis, since the data set collected for each aircraft event was only referenced to itself, not to an aircraft group.

Of 339 total departures collected during the seven days of measurements, 237 events were recorded for the six primary aircraft types listed above. Of these 237 events, 45 met the wind and climb gradient criteria and were retained for final analysis. The retained data are shown in Fig. 4. This shows the 45 retained aircraft events with 5 data points for each event. The data points are plotted as a function of elevation angle. The residual may possibly contain meteorological effects, but retaining only data for which wind speeds were

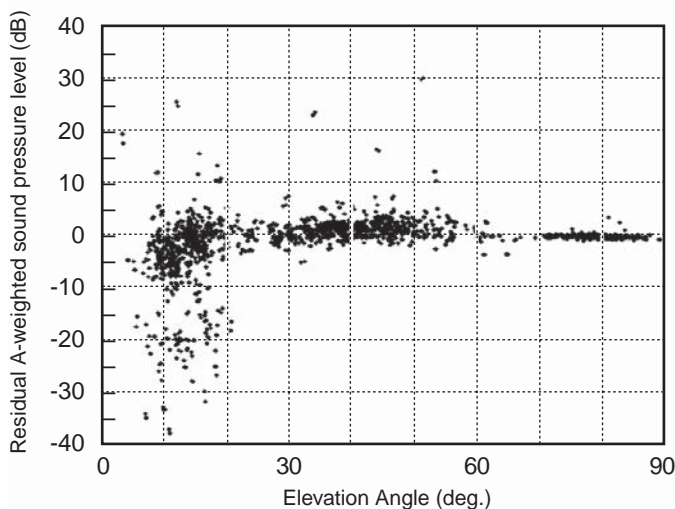


Fig. 3 – All departure data.

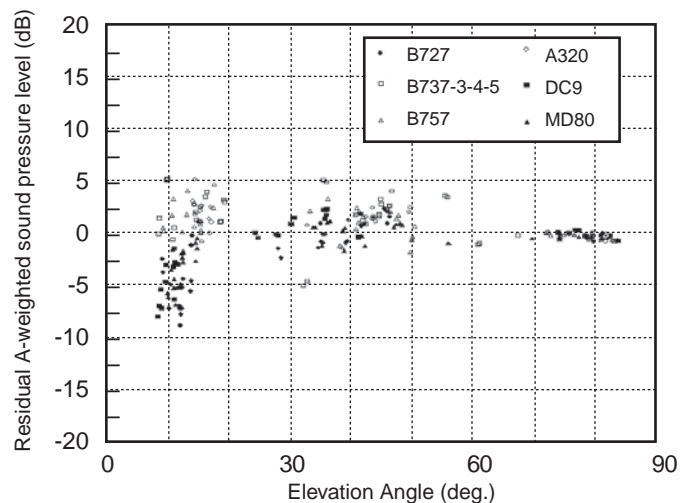


Fig. 4 – Retained departure data.

less than 16.1 km/hr (10 mph) should eliminate the majority of these effects. The data tend to cluster in three groups. The data cluster between 8 and 20 degrees was from Corinha Beach, the data cluster from 20 to 60 degrees was from Snake Island, and the data cluster above 60 degrees was from Pt. Shirley.

5. DATA ANALYSIS

This section presents an analysis of the retained data. The first step in the analysis was to confirm that no problems existed with the signal-to-noise ratio of the measurements collected at Corinha Beach, the most distant measurement site from the nominal tracks. The second step was to examine the value of the ground flow resistivity used for correcting data measured at the Pt. Shirley site. For the two over-water propagation measurement sites, a flow resistivity of 20,000 c.g.s rayls was used. A statistical analysis was then performed to examine the differences between aircraft types based on engine location. Finally, an examination of the installation effects as a function of one-third octave-band frequency for all types of aircraft was conducted.

A. Signal-to-noise ratio at Corinha Beach

Signal-to-noise ratio is the ratio of the desired signal to the ambient or background levels which interfere with the measurement of the desired signal. At a minimum, a desired signal should be 10 dB greater than the background levels. With a 10 dB rise above the noise floor, the error in the signal due to the background levels can be neglected. Analysis showed that at the most distant Corinha Beach site, even the quieter Stage 3 aircraft such as the B757 had a maximum A-weighted sound level about 15 dB, and an LCPA of about 12 dB, above the background level. Consequently, it was concluded that signal-to-noise ratio was not an issue in the current study.

B. Ground flow resistivity at Pt. Shirley

The ground cover at Pt. Shirley was closely mowed grass. For this type of ground cover, a range of flow resistivities between 150 and 300 c.g.s. rayls is recommended by Embleton, et al.¹² The results of using these flow resistivities to correct the data measured at the 1.5 m reference microphone were examined. The only noticeable difference occurred at the half-wavelength interference frequency of 63 Hz. For an A-weighted analysis, this difference was effectively negligible. For all further analysis, the flow resistivity of 150 c.g.s. rayls was used.

C. Statistical analysis by engine location

Examination of Fig. 4 shows that data measured for different aircraft types tend to cluster based on engine location. This is particularly noticeable at the lower elevation angles observed from Corinha Beach. Fig. 4 displays the data for those aircraft with tail-mounted engines (B727, MD80, DC9) as closed symbols and the data for those aircraft with wing-mounted engines (B737 with CFM series engines, B757,

A320) as open symbols. The rest of this section presents a separate analysis of the data based on these two groups of aircraft.

Figure 5 shows the three aircraft types with tail-mounted engines as a separate group from the entire set of data shown in Fig. 4. An exponential regression line has been drawn through the data to enable the reader to better view the trend in the data. The residual effect for these aircraft is pronounced between 8 and 20 degrees of elevation.

As stated in Section 1B, one of the primary objectives of this study was to quantify the error associated with the use of SAE AIR 1751. A further objective was to compare the data measured in the current study with data measured in a similar study conducted by the National Air Traffic Services, Ltd (NATS).

Figure 6 shows the difference between the SAE AIR 1751 equation for lateral attenuation and the data measured at Logan for the B727 aircraft. The figure also shows the 95% confidence intervals of the best linear fit through the data. At high and low angles, the confidence intervals encompass zero, indicating there is no statistically significant difference between the Logan data and the SAE AIR 1751 equations for the B727 at these angles. Between about 20 and 50 degrees, a statistically significant difference does appear between the Logan data and the SAE AIR 1751 equations. However, the difference is on the order of a few tenths of a decibel. The agreement between the Logan B727 data and the SAE AIR 1751 equation was expected since, as mentioned previously, the SAE AIR 1751 data set is dominated by the B727 aircraft.

To determine if a statistically significant difference between the NATS curve and the data collected at Logan exists, the differences between the NATS curve and the Logan data were plotted as a function of elevation angle. The 95% confidence intervals (CI) for these differences were then calculated. Figure 7 shows the results of these calculations. The best linear fit of the difference is slightly less than one dBA for all elevation angles. At all angles, the lower CI line is very close to encompassing the zero line. Although the two data sets are not statistically equivalent at all elevation angles, the differences are small.

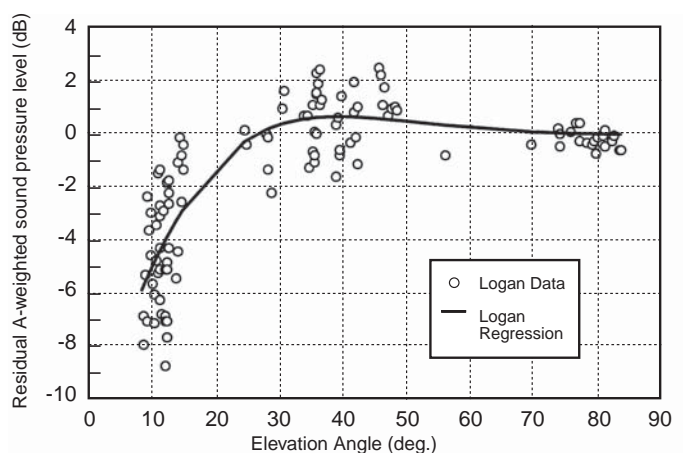


Fig. 5 – Regression through Logan data (tail-mounted engines).

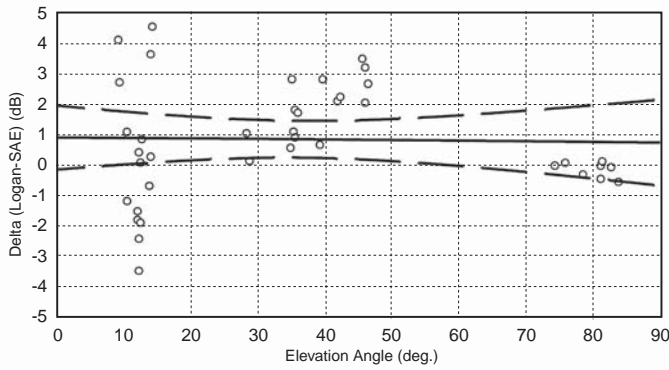


Fig. 6 – Difference between B727 data and SAE AIR 1751 regression (tail-mounted engines).

Figure 8 shows the three aircraft types with wing-mounted engines as a separate group. A “trend line” has been drawn through the Logan data at the lower elevation angles to enable the reader to better view the general behavior of the data. This trend line is the arithmetic average of the data at angles below 60 degrees. The residual effect for these aircraft is the opposite of the tail-mounted engine group. For these aircraft an *augmentation* at the lower elevation angles is observed; the noise measured for these aircraft is higher than what would be measured directly under the aircraft at the same slant distance. For elevation angles below 60 degrees, this augmentation appears independent of elevation angle. For comparative purposes, the lateral attenuation curve from SAE AIR 1751 and the lateral attenuation curve generated by NATS for these aircraft types are also shown in Fig. 8.

A statistical comparison between the Logan results for the aircraft with wing-mounted engines and the SAE AIR 1751 and the NATS lateral attenuation curves was not performed since the differences were so substantial, and a comparison was considered unnecessary. Although the NATS curve showed similar augmentation between 20 and 60 degrees as compared with the Logan data, the data differ substantially at the lower elevation angles. In addition, the difference between the Logan data and the SAE AIR 1751 curve of approximately 4 dB at the mid-angles and 8 dB at

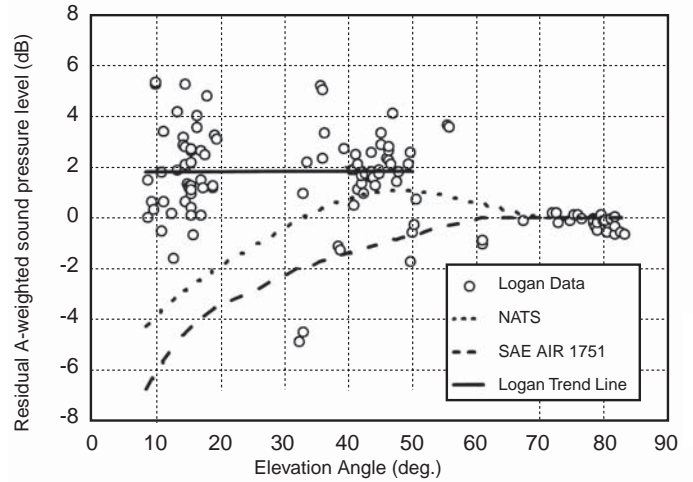


Fig. 8 – Comparison of trends/regression (wing-mounted engines).

the low angles should be noted. These large differences at low angles for aircraft with wing-mounted engines imply that noise prediction models that use the existing lateral attenuation algorithms may be under-predicting the noise generated by these aircraft by a similar magnitude.

D. Installation effects as a function of frequency

Finally, an examination of the installation effects as a function of one-third octave-band frequency for all types of aircraft was conducted. Figure 9 shows, for elevation angles between 8 and 20 degrees, the average residual effect for the six retained aircraft types as a function of frequency for frequencies between 250 Hz and 4000 Hz. Because of the nature of A-weighting, these frequencies dominate all of the analyses presented herein. As can be seen, there is a clear distinction between the wing-mounted and tail-mounted aircraft. Figure 9 also shows that the installation effect is not a strong function of frequency for these six aircraft types. This relative lack of frequency dependence for each of the six types is a further indicator that signal-to-noise was not a factor, and, more importantly, that a significant difference in residual exists between aircraft with tail-mounted and wing-mounted engines.

E. Additional observations

The first topic in this section is an overview of the differences in aircraft geometries, and how these differences may help explain the figures presented above. The second topic in this section examines the correlation between the L_{CPA} and SEL data measured in this study.

F. Geometry of aircraft

The data presented above showed significant differences in the engine installation component of lateral attenuation between aircraft with wing-mounted engines and aircraft with tail-mounted engines. Possible reasons for these differences are related to the differences in physical geometry of these two groups of aircraft.

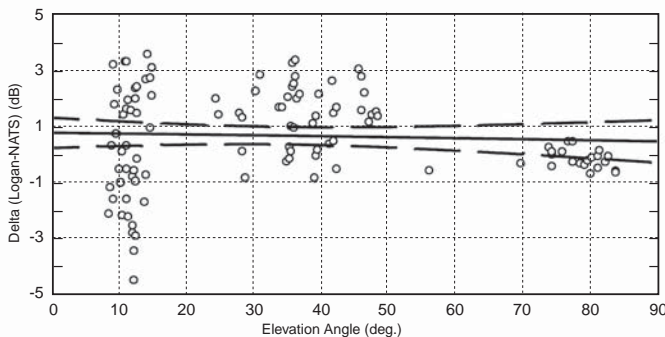


Fig. 7 – Difference between Logan Data and NATS regression (tail-mounted engines).

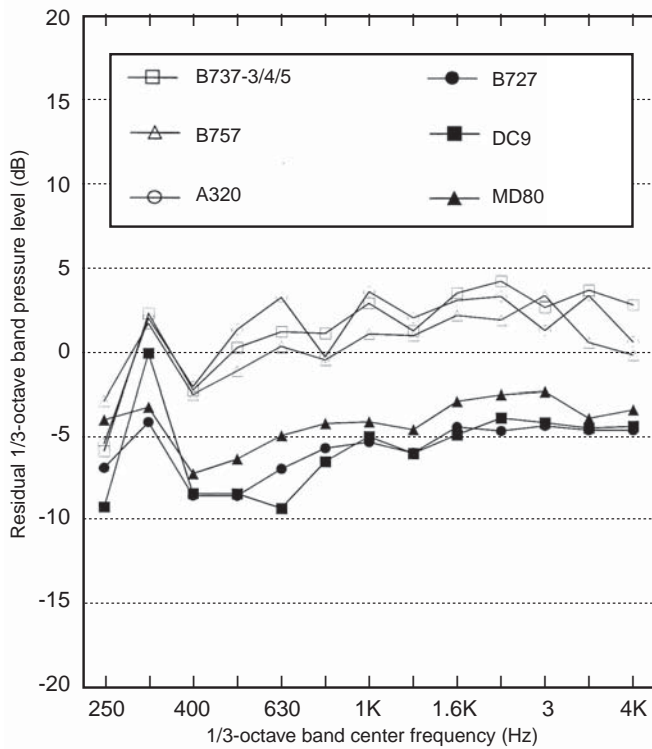


Fig. 9 – Residual as a function of frequency (elevation angles from 8 to 20 degrees).

Noise generated by jet engines has a number of discrete sources. These discrete sources include the fan, the compressor and turbine machinery, the combustor, and primary (jet) and secondary (fan) exhausts. These noise sources tend to be directional. The fan noise generally propagates forward, the machinery and combustor noise propagates perpendicularly, and the exhaust noise tends to propagate to the rear.¹³ Because this study examined noise observed at CPA, fan noise and exhaust noise are probably not major factors in the residuals presented in Section 5.C.

When aircraft with tail-mounted engines are perpendicular to the receiver at low angles (8 to 20 degrees), the farthest engine is completely shielded by the fuselage or the vertical stabilizer. With complete shielding of the farthest engine(s), the noise would be reduced up to 3 dB ($10\log(1/2) = -3$) for a two-engine aircraft and up to 4.8 dB ($10\log(1/3) = -4.8$) for a three-engine aircraft in the limiting case of closely-spaced, co-linear engines. Hodge has noted that additional attenuation may be due to aerodynamic flow-field effects.¹⁴ These effects are the scattering of the engine noise as it passes through the wing down-wash and the wingtip vortices. These effects, combined with some shielding of the farthest engine(s), may account for the residual at low angles seen in Fig. 5.

For aircraft with tail-mounted engines at mid-range elevation angles (20 to 60 degrees), the farthest engine may be visible under the fuselage. As such, the aircraft with tail-mounted engines tend to show an augmentation similar to the aircraft with wing-mounted engines (Figs. 5 and 8, respectively). This augmentation for aircraft with tail-mounted engines may be due to the combination of the incomplete

shielding of the farthest engine and the reflection of the noise from the closest engine off the relatively flat horizontal and vertical stabilizers.

Modern jet aircraft with wing-mounted engines do not have constant chord wings, but rather have a significant taper ratio. The taper ratio is highest between the engine and the fuselage, where the leading edge of the wing is swept while the trailing edge projects almost perpendicular to the fuselage. This means the engine farthest from the receiver has a fairly broad and flat surface from which to reflect noise.

For the three types of aircraft with wing-mounted engines included in this report, the engines are either forward or under the wing. These locations provide limited opportunity for noise from the closest engine to reflect off aircraft surfaces. In addition, these locations provide limited opportunity for noise from either engine to be shielded by the fuselage. However, as mentioned above, noise from the farthest engine could possibly reflect off the underside of the fuselage and the wing center section. These reflections may account for the augmentation at elevation angles below 60 degrees shown in Fig. 8. Conversely, the lack of any apparent residual as a function of angle in this figure indicates that aerodynamic flow-field effects may be negligible for aircraft with wing-mounted engines.

In addition, the residual augmentation seen in Fig. 8 for aircraft with wing mounted engines may be due to assumed perfectly straight source-to-receiver paths that, in fact, were not. Figure 10 presents an example of modeled ground effect as a function of reflection angle. The figure is based on the EPD ground effects model used in this study. The figure represents a ground distance of 1000 meters between the source and the receiver, which is the nominal CPA distance from Corinha Beach. The figure shows a ground effect of about three decibels when reflection angles are less than about one degree and less than one decibel when reflection angles are above about 10 degrees. The combined average ground effect based on the EPD model for the aircraft observed from Snake Island and Corinha Beach is 0.57 decibels. If the source-to-receiver sound path was curved (possibly from slight wind or

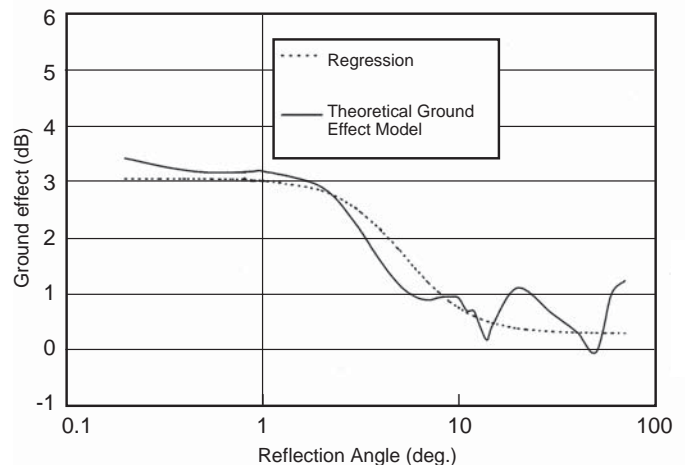


Fig. 10 – Ground effect on 1000 meters (based on EPD model).

temperature gradients), the actual reflection angle could be slightly lower than was assumed with straight-path propagation. The effect of applying this lower reflection angle (and increased ground effect) would be to reduce the residual augmentation. This residual augmentation may also be inherent in the data for aircraft with tail-mounted engines. Lower actual reflection angles could be possibly caused by the effects of water surface conditions on the propagation path and/or micro-meteorological effects at the water/air boundary.¹⁵ Investigation of these factors is beyond the scope of this study.

G. Relationship of L_{CPA} and integrated metrics

The ability to accurately track aircraft, and to coordinate that tracking information with acoustic data was an important component of this study. Most uncontrolled aircraft noise studies conducted to date have not had the luxury of this precise coordination, and so have relied on integrated noise metrics such as SEL and/or DNL. Integrated metrics correlate with community response to aircraft noise, and provide a useful comparison of noise levels, but they do not allow close dissection of individual components of aircraft noise. One of the problems with integrated metrics is that they can include noise energy generated during different aircraft configurations, e.g., flap and power settings. For example, an SEL metric for a departure will generally contain all the aircraft noise generated during a period in which the noise of the aircraft is within 10 dB of the maximum noise generated by the aircraft. This period will, by definition, contain the noise produced over a range of directivity angles and slant distances. The period may also contain noise from different aircraft configurations such as power setting changes or flap changes.

Although the SEL metric may not be as precise a tool as the L_{CPA} metric for examining the details of aircraft noise, examination of the data collected at Logan showed a high correlation between L_{CPA} and SEL. For measurements made at Corinha Beach, the correlation is shown in Fig. 11. For the equation $SEL=14.2+0.99L_{CPA}$ the correlation coefficient is 0.92. The SEL was calculated using noise data above the 10dB down points. Future analysis will include more detailed examination of the SEL metric.

For measurements made at Pt. Shirley, the correlation is shown in Fig. 12. For the equation $SEL=8.0+L_{CPA}$, the correlation coefficient is 0.92.

The data shown in Figs. 11 and 12 used to generate the corresponding equations were based on the B727 and B757 aircraft only. These are the two most common types of aircraft in each of the sub-groups examined. Also, although a correlation exists at each site, no conclusions can be drawn that the SEL data at Corinha Beach correlates with the SEL data at Pt. Shirley. The methods of correcting the data from Corinha Beach to the reference microphone at Pt. Shirley relied on knowing the exact aircraft location and spectra at each moment in time. This information is lost in the SEL metric. Despite this caveat, the high correlation between the SEL and L_{CPA} descriptors may indicate that the conclusions of this study would not change if SEL were selected as the metric of analysis.

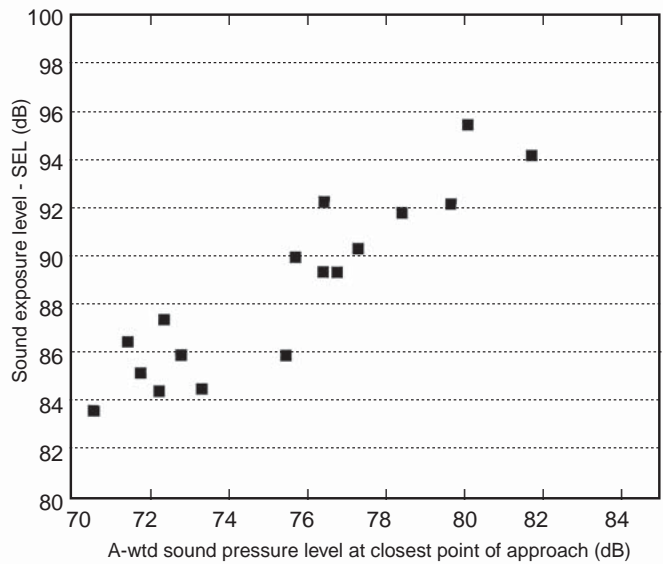


Fig. 11 – L_{CPA} versus SEL at Corinha Beach.

6. CONCLUSION AND RECOMMENDATIONS

Based on the analysis of the data collected at Logan, the following conclusions are made:

- The ground effects algorithms based on the work of Embleton, Piercy and Daigle appear reasonable for A-weighted metrics.¹² These algorithms produce the expected results at overhead angles, where the reference microphone and the associated 4.5 m microphone correct to essentially the same A-weighted values.
- Lateral attenuation/installation effects for the aircraft with tail-mounted engines substantially agree with SAE AIR

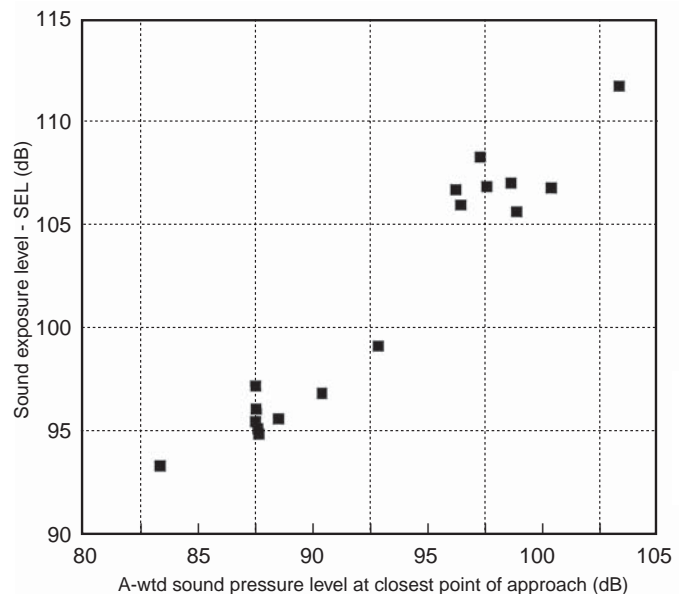


Fig. 12 – L_{CPA} versus SEL at Pt. Shirley.

1751 and data recently collected by NATS in the U.K.

- Significant differences exist between aircraft with wing-mounted engines and SAE AIR 1751. For the flight track measurement geometries in this study, aircraft with wing-mounted engines had a lateral *augmentation*, not an attenuation. The data collected in the current study for aircraft with wing-mounted engines also differ from data recently collected by NATS in the U.K., especially at elevation angles below about 20 degrees.
- Because aircraft with wing-mounted engines have become much more predominant in the fleet since SAE AIR 1751 was developed, inclusion of updated lateral attenuation algorithms for these aircraft in the next generation of noise models will result in substantial improvement in model accuracy as well as an increase in the areas of the predicted noise contours.

Before SAE AIR 1751 can be modified, more data are required to help understand the differences observed in the current study compared with the recent studies conducted by NATS. These data should be collected in an environment where all aircraft parameters can be controlled. The metrics used in such a data collection effort should be the same as those used in the standard noise models that would make use of such data. Further, since relatively good agreement has been obtained for aircraft with tail-mounted engines, this additional work should focus on aircraft with wing-mounted engines.

7. ACKNOWLEDGMENTS

The authors gratefully acknowledge the support of the Structural Acoustics Branch of the National Aeronautics and Space Administration (NASA) Langley Research Center (LaRC), especially Dr. Kevin P. Shepherd, the NASA technical monitor.

8. REFERENCES

- ¹ Society of Automotive Engineers, Committee A-21, Aircraft Noise, "Prediction method for lateral attenuation of airplane noise during takeoff and landing," Aerospace Information Report No. 1751 (Society of Automotive Engineers, Inc., Warrendale, Pennsylvania, March 1981).
- ² W. L. Willshire, "Lateral attenuation of high-by-pass ratio engines aircraft noise," NASA Technical Memorandum 81968 (NASA, Hampton, VA, 1981).
- ³ J. D. Speakman and B.F. Berry. "Modeling lateral attenuation of aircraft flight noise;" Proc. INTER-NOISE 92, edited by Giles A. Daigle and Michael R. Stinson (Noise Control Foundation, Poughkeepsie, New York, 1992).
- ⁴ Engineering Science Data Unit (ESDU), "Lateral attenuation calculations," ESDU AN66, London, April 1990.
- ⁵ D. E. Bishop and J.M. Beckmann. "Study of Excess Sound Attenuation as Determined From Far Part 36 Aircraft Noise Certification Measurements," BBN Report No. 4219 (Bolt Beranek and Newman, Cambridge, Massachusetts, May 1980).
- ⁶ John Gulding, et. al. "Integrated Noise Model (INM) version 6.0 User's Guide," Report No. FAA-AEE-99-03 (Federal Aviation Administration, Washington, D.C., December 1996).
- ⁷ Gregg G. Fleming, et. al. "Integrated Noise Model (INM) Version 5.1 Technical Manual," Report No. FAA-AEE-97-04 (Federal Aviation Administration, Washington, D.C. 1997).
- ⁸ M. J. T. Smith, et. al., "Development of an Improved Lateral Attenuation Adjustment for the UK Aircraft Noise Contour Model," ANCON, DRAFT, R&D report 9953 (Department of Operational Research and Analysis, National Air Traffic Services Ltd., London, November 1999).
- ⁹ G.G. Fleming, J. Burstein, A. S. Rapoza, D. A. Senzig, and J. M. Gulding, "Ground effects in FAA's integrated noise model," Noise Control Eng. J. **48**(1), 16-24 (2000).
- ¹⁰ D. A. Senzig, G. G. Fleming, and J. P. Clarke, "Lateral Attenuation of Aircraft Sound Levels Over an Acoustically Hard Water Surface: Logan Airport Study," NASA Report No. NASA/CR-2000-210127 (National Aeronautics and Space Administration, Washington, D.C., May 2000).
- ¹¹ G. G. Fleming, C. J. Roof, J. Ruggiero, M. Geyer, B. Kim, T. Connor, and J. Skalecky, "A differential global positioning system for determining time space position information in support of aircraft noise certification," Proc. 2001 National Technical Mtg., Inst. of Navigation (2001).
- ¹² Tony F. W. Embleton, Joe E. Piercy, and Giles A. Daigle, "Effective flow resistivity of ground surfaces determined by acoustical measurements," J. Acoust. Soc. Am. **74**(4), 1239-1243 (1983).
- ¹³ Noel A. Peart, et. al., Flyover-Noise Measurement and Prediction, in *Aeroacoustics of Flight Vehicles, vol. 2: Noise Control*, edited by Harvey H. Hubbard (Acoustical Society of America, Melville, N.Y., 1995), pp. 357-382.
- ¹⁴ Charles G. Hodge, Quiet Aircraft Design and Operational Characteristics, in *Aeroacoustics of Flight Vehicles, vol. 2: Noise Control*, edited by Harvey H. Hubbard (Acoustical Society of America, Melville, N.Y., 1995), pp. 383-414
- ¹⁵ H. U. Roll, *Physics of the Marine Atmosphere* (Academic Press, New York, 1965).